C.P. No. 116
(15,595)
A.R.C. Technical Report

MINISTRY OF SUPPLY

AERONAUTICAL RESEARCH COUNCIL

CURRENT PAPERS

Charts of the Wave Drag of Wings at Zero Lift

By

T. Lawrence, B.Sc., B.E.

LONDON: HER MAJESTY'S STATIONERY OFFICE

1953

Price 3s. 6d. net

C.P. No. 116

Technical Note No. Aero 2139 Revised

November, 1952.

ROYAL AIRCRAFT ESTABLISHMENT

Charts of the wave drag of wings at zero lift

by

T. Lawrence, B.Sc., B.E.

SUMMARY

Theoretical calculations of the wave drag at supersonic speeds of nonlifting wings of double wedge and biconvex section are reviewed, and the best method of presenting the results considered. Using this method, a representative selection of the available numerical evaluations of the theory, are presented. These should be of value for wing drag estimation purposes.

[This is a revised version of the note published in January 1952. Figs. 3(b), 3(c) and 6(b) are additional. The original Figs. 4 and 5 were obtained by crossplotting from Ref.17; an attempt was made to extend the curves to $A\sqrt{M^2-1} = \frac{1}{2}$ using Margolis' equations (Ref.6) and this revealed discrepancies in the curves at low $A\sqrt{M^2-1}$, due to the small scale of Chang's original charts. The present Figs. 4 and 5 are obtained by calculation from Margolis' equations until agreement with the original curves was obtained, as explained in the text. Fig.8 is redrawn from the new Figs. 4 and 5, and Fig. 9(b) is additional. Some minor editorial corrections were necessary to make the note self-consistent.]

LIST OF CONTENTS

1 Introduction

Since Jones[1] and Puckett[2] first produced their source distribution methods for the solution of the wave drag of thin, nonlifting wings in supersonic flow, there has been a steady growth in the number of different, more particular cases, for which the theory has been worked out. These results are widely scattered, there is considerable overlap so that it is not always easy to find the analytical solution for a particular case, nor is it immediately apparent just which particular solutions have been evaluated quantitatively.

A further difficulty is that there is not as yet a universally accepted method of presenting the results of such calculations. Comparison of the results of calculations by different authors frequently involves some replotting, whilst comparisons of theory and experiment may necessitate determining the theoretical curve by cross-plotting from a number of different charts. The charts that are available on the whole have been prepared to display graphically the behaviour of the analytical solutions and pay insufficient attention to the physical significance of the results, for example they cover combinations of sweep and aspect ratio beyond any magnitudes being contemplated for even the most advanced designs of the future at the expense of cramping the curves in the more practical regions.

This note is an attempt to systematise this particular aspect of supersonic wing theory by

(a) Considering the best method of displaying the results graphically,

(b) Replotting in this chosen form existing evaluated solutions for the wave drag of nonlifting wings,

(c) Surveying the field covered by (b) to see what additional numerical evaluations should be undertaken.

2 Method of presentation

The wave drag of a wing of simple planform (Fig.1) and uniform section may be expressed in the functional form

$$C_D = f\{\tau, M, A, \Lambda, \lambda\}$$

where C_D = wave drag co-efficient, based on plan area

τ = thickness/chord ratio, t/c, assumed constant across the span

M = free stream Mach number

A = aspect ratio

Λ = sweep of a characteristic spanwise line

λ = taper ratio.

Now theory indicates that the functional dependence upon τ is simply that C_D varies as τ^2, and further, the similarity law shows that the dependence upon M can be absorbed into the dependence upon the geometrical parameters, so that the functional form becomes

$$\frac{\sqrt{M^2-1}}{\tau^2} \cdot C_D = f\{A\sqrt{M^2-1}, \cot\Lambda\sqrt{M^2-1}, \lambda\}$$

It is believed that the charts will be of most general use if they contain lines which represent the drag of given wings, over a range of M, rather than lines which show the effect on drag of changing one or more of the geometrical parameters. For this reason it is suggested that Mach number should appear in only one of the parameters, and that the curves should be plotted against this parameter. This can be accomplished by rewriting the functional expression for C_D in the form

$$\frac{C_D}{A\tau^2} = f\{A\sqrt{M^2-1},\ A\tan\Lambda, \lambda\}.$$

We have, therefore, chosen to plot $\frac{C_D}{A\tau^2}$ against $A\sqrt{M^2-1}$ for constant $A\tan\Lambda$ and λ, and to prepare a separate diagram for each λ. Further, $\frac{C_D}{A\tau^2}$ is plotted logarithmically, to cover a wide range with uniform accuracy.

We have also to consider which line of sweep we are to use to define Λ, and the choice has fallen on the half-chord line, because this line gives the best measure of the "average" sweep of a wing. A wing having a high degree of sweep on the leading edge, but little or no sweep on the trailing edge (a delta, for example) only exhibits the features of moderate sweep in its aerodynamic characteristics. This can be allowed for by considering the half-chord sweep. Further, half-chord sweep has been used as the basis for other aerodynamic parameters, lift curve slope and aerodynamic centre, for example. The use of maximum thickness sweep is ruled out by the fact that it does not depend solely upon the planform but involves in addition a knowledge of the sectional shape. The sweep of the half-chord line will be denoted by $\Lambda_{\frac{1}{2}}$.

The method of presentation chosen has the following advantages

(a) it is a plot basically of C_D v M,

(b) C_D, M and $\Lambda_{\frac{1}{2}}$ appear only once each in the parameters, so that the variations with M and $\Lambda_{\frac{1}{2}}$ can be seen readily,

(c) the curves are conveniently spaced on the chart and linear interpolation is facilitated,

(d) the percentage accuracy with which the ordinate of any curve can be read is constant.

The diagrams contain lines of constant $A\tan\Lambda_{\frac{1}{2}}$ in intervals of unity from 0 to 6, which is considered to cover the range of greatest present interest, and go up to $A\sqrt{M^2-1} = 7$, which in general puts the leading edge supersonic.

If we consider the basic geometry of a swept tapered wing (Fig.1), then several fundamental relationships may be derived.

$$\frac{1-\lambda}{1+\lambda} = \tfrac{1}{2} A\tan\Lambda_o \cdot \frac{1-\sigma}{2}$$

and

$$\frac{\tan\Lambda_r}{\tan\Lambda_o} = 1 - r(1-\sigma)$$

where σ = sweep ratio = $\dfrac{\tan \Lambda_1}{\tan \Lambda_o}$

r = position of any line aft of leading edge - fraction of chord.

Now the spanwise line distant rc behind the leading edge, and having sweep Λ_r is sonic when

$$A\sqrt{M^2-1} = A \tan \Lambda_r .$$

Hence the leading edge is sonic when

$$\begin{aligned} A\sqrt{M^2-1} &= A \tan \Lambda_o \\ &= A\left[\tan \Lambda_{\frac{1}{2}} + \tfrac{1}{2}\, c.\, \frac{1-\sigma}{c} \tan \Lambda_o\right] \\ &= A \tan \Lambda_{\frac{1}{2}} + 2.\left(\frac{1-\lambda}{1+\lambda}\right), \end{aligned}$$

the trailing edge is sonic when

$$\begin{aligned} A\sqrt{M^2-1} &= A \tan \Lambda_1 \\ &= A \tan \Lambda_{\frac{1}{2}} - 2\left(\frac{1-\lambda}{1+\lambda}\right), \end{aligned}$$

and the line of maximum thickness is sonic when

$$\begin{aligned} A\sqrt{M^2-1} &= A \tan \Lambda_m \\ &= A\left[\tan \Lambda_{\frac{1}{2}} + (\tfrac{1}{2}-m)\, c.\, \frac{1-\sigma}{c} \tan \Lambda_o\right] \\ &= A \tan \Lambda_{\frac{1}{2}} + 4\,(\tfrac{1}{2}-m)\left(\frac{1-\lambda}{1+\lambda}\right). \end{aligned}$$

The main characteristics of each family of curves for a wing of symmetrical double wedge section* are shown in Fig.2. Each curve refers to a family of wings of constant λ, m and $A \tan \Lambda_{\frac{1}{2}}$, derived from one another by stretching the planform spanwise at constant chordwise tip position as illustrated in the inset diagram. Curves to the left of each figure refer to wings of low $A \tan \Lambda_{\frac{1}{2}}$, and curves to the right to wings of high $A \tan \Lambda_{\frac{1}{2}}$, derived as illustrated by shearing the tip chordwise at constant spanwise tip position.

---

* In the past the term "symmetrical double wedge" has been used to refer to a diamond shaped or doubly symmetrical section i.e. one that is both symmetrical with respect to the chord line, and has the maximum thickness position at mid-chord. By anology with aerofoil section terminology, we here use the term "symmetrical" as synonymous with "uncambered" and leave the maximum thickness position to be further specified.

Now peaks (discontinuities in the slope) occur in the drag curves whenever changes arise in the flow pattern e.g. when any line of discontinuity in the slope of the section (such as leading and trailing edges) becomes sonic, and when the Mach line from any change in planform crosses any other change in planform (such as the Mach line from the leading edge of the root chord crossing the trailing edge of the tip chord). On wings of symmetrical double wedge section, for which most of the theory has been worked out, there are three major peaks, respectively when the trailing edge, maximum thickness line and leading edge become sonic. As shown in Fig.2, they are spaced from one another by a constant interval in $A\sqrt{M^2-1}$. For aerofoil sections the peak when the maximum thickness line becomes sonic disappears. When λ is not zero, the peaks due to changes in planform become very numerous but quite small in magnitude; Figs. 6,8 indicate their magnitude in the particular case of an untapered wing of symmetrical double wedge section ($\lambda = 1.0$, $m = 0.5$). These minor peaks are ignored in all other cases.

3 Summary of Calculations

3.1 Wedge Profiles

3.11 Fully tapered planforms - $\lambda = 0$ Fig.3

Puckett's original work[2] considered a delta wing of symmetrical double wedge profile ($m = 0.5$), and later, with Stewart[8] this was extended to cover other fully tapered planforms, and maximum thickness positions. The solutions were evaluated only for $A \tan \Lambda_{\frac{1}{2}}$ equal to 6 and 2. The solutions apply for both "subsonic" and "supersonic" conditions. Neilson[9] dealt with the unswept wing ($A \tan \Lambda_{\frac{1}{2}} = 0$) while Kleissas[5] considers a limited region with a "subsonic" leading edge. Both these authors give their results in chart form. Multhopp and Winter[13] prepared charts from which, with some labour, the drag of any fully tapered wing can be determined.

All these results have been compared, and no major discrepancies detected. Figs. 3(a), 3(b) and 3(c) have been calculated from Multhopp and Winter for large values of $A\sqrt{M^2-1}$, and the values at $A\sqrt{M^2-1} = 0$ were obtained by taking a limiting case of the results in Ref.8.

Multhopp and Winter's charts can be applied to a fully tapered planform of multiple wedge profile having any combination of flats, but the application becomes increasingly laborious.

3.12 Tapered planforms $0 < \lambda < 1.0$ Figs. 4,5

Margolis treated the tapered wing in the fully subsonic case (trailing edge subsonic) in Ref.6 and later (Ref.11) extended this to the case when the trailing edge is supersonic. In neither reference has any general numerical evaluation of the solutions been attempted. Kleissas[5] has again done some limited evaluation for $\lambda = \frac{1}{4}, \frac{1}{3}, \frac{1}{2}, \frac{3}{4}$ and Chang[17] has produced both an analytical solution and an evaluation for $\lambda = 0.2$ and 0.5. Neilson[9] has evaluated the unswept wing drag for $\lambda = \frac{1}{4}, \frac{1}{2}, \frac{3}{4}$.

All these results are for a mid-chord position of the maximum thickness ($m = 0.5$), and there are no inconsistencies where they overlap. Chang's spacing in λ of 0 : 0.2 : 0.5 : 1.0 gives 1 : $\frac{2}{3}$: $\frac{1}{3}$: 0 in $(1-\lambda)/(1+\lambda)$ i.e. a linear spacing and (see Fig.8) the curves are nearly linearly spaced, making interpolation easier; this spacing is adopted. Figs. 4 and 5 are cross-plotted from Chang's curves for values

of $A\sqrt{M^2-1}$ greater than that at which the trailing edge becomes sonic. For a completely subsonic wing Chang's curves are on too small a scale to allow reliable cross-plotting, and the curves were computed from Margolis' theory (Ref.6).

3.13 Untapered planforms $\lambda = 1.0$ Fig.6

Jones[1] considered this case originally, but gave no evaluations. Bonney[3] considered the unswept wing, again purely from the analytical aspect; Kleissas[5] did some limited evaluation. Neilson[9] gives an evaluation for the unswept wing. Margolis[10] considered the effect of maximum thickness position on drag and evaluated the result for one planform. From a computing point of view, this treatment is the most convenient and has been used to derive Figs. 6(a) and 6(b) for $m = 0.5$ and 0.3 respectively. Comparison will show that the effect of m is small and almost confined to the "supersonic" region; the curve for $m = 0.4$ is not reproduced.

In these figures the minor peaks referred to in paragraph 2 above have been reproduced in their entirety, to show their magnitude. In the case of tapered wings they will be of relatively smaller magnitude (i.e. smaller deviation from the smooth curve) disappearing completely for the fully tapered wing.

3.2 Biconvex profiles

3.21 Fully tapered planforms - $\lambda = 0$

Beane[16] has dealt with a circular arc* biconvex section by approximating with a multisided polygon. However the application is limited and there are no significant evaluations. No curves are reproduced.

3.22 Tapered planforms $0 < \lambda < 1.0$

Beane again has dealt with this case, but only when the wing is purely supersonic. Kainer[12] has considered the tapered planform of parabolic arc* biconvex section, and evaluated his result for one wing of $\lambda = 0.531$, $m = 0.5$, $A \tan \Lambda_m = 2.76$, at $A\sqrt{M^2-1} = 4.64$.

3.23 Untapered planforms $\lambda = 1.0$ Fig.7

Harmon and Swanson[4,7] have computed the drag of the untapered wing of parabolic arc* biconvex section. The results are given in Fig.7.

3.3 Effect of Taper

In Fig.8 we have cross plotted, from Figs. 3(a), 4, 5 and 6(a) the curves for wings of $A \tan \Lambda_{\frac{1}{2}} = 4, m = 0.5$. It will be seen that there are slight inconsistencies in the curves; this is not surprising considering their origins and the sizes of diagram from which Figs. 4,5 have been crossplotted. No attempt is made to remove these discrepancies by making the curves self consistent, but the inconsistencies are allowed to remain as an indication of the accuracy of the Figures. Otherwise the curves are fairly linearly spaced in $(1-\lambda)/(1+\lambda)$ as pointed out previously, which should make interpolation easier.

3.4 Effect of Maximum thickness position

In Fig. 9(a) is shown the effect of maximum thickness position on the drag of fully tapered wings, for two planforms[8]. The fact that the

---

* Within the accuracy of the theory dealt with in these cases there is no difference between circular arc and parabolic arc biconvex sections.

ordinate change for a given change in m is fairly constant when the wing is fully subsonic or fully supersonic, gives a useful lead on interpolation.

For untapered wings, the effect is shown in Fig.9(b). Nonweilor[14] and Shaw[15] have made preliminary studies for the case where $0 < \lambda < 1$.

4 Developments

The most immediate need is for a comparison of these theoretical results with actual measurements of the drag of representative wings. This work is in hand. It should give some information how best to estimate the drag of wings of round nose section, which are of immediate practical interest. It may reveal the need for more charts to supplement Figs. 4 and 5, although they can probably be derived with sufficient accuracy by interpolation between Figs. 3 and 6.

5 Notation

A	aspect ratio
C_D	wave drag coefficient
M	Mach number
mc	position of maximum thickness line aft of leading edge
λ	taper ratio = tip chord/root chord
Λ_o	sweepback of leading edge
Λ_m	sweepback of maximum thickness line
$\Lambda_{\frac{1}{2}}$	sweepback of half chord line
Λ_1	sweepback of trailing edge
σ	sweep ratio = $\tan \Lambda_1 / \tan \Lambda_o$
τ	thickness/chord ratio

REFERENCES

No.	Author	Title, etc.
1	Jones	Thin oblique aerofoils-at supersonic speeds NACA TR No.851 (NACA TN No.1107) September, 1946
2	Puckett	Supersonic wave drag of thin aerofoils J.Ae.Sci. Vol.13 No.9 p.475 September, 1946
3	Bonney	Aerodynamic characteristics of rectangular wings at supersonic speeds J.Ae.Sci. Vol.14 No.2 p.110 February, 1947

REFERENCES(Contd.)

No.	Author	Title, etc.
4	Harmon and Swanson	Calculations of the supersonic wave drag of non-lifting wings with arbitrary sweepback and aspect ratio NACA TN No.1319 (TIB/1117) 1947
5	Kleissas	Charts of the zero-lift drag of supersonic sweptback wings for various aspect ratios September, 1947
6	Margolis	Supersonic wave drag of sweptback tapered wings at zero lift NACA TN No.1448 (TIB/1189) October, 1947
7	Harmon	Theoretical supersonic wave drag of untapered sweptback and rectangular wings at zero lift NACA TN No.1449 October, 1947
8	Puckett and Stewart	Aerodynamic performance of delta wings at supersonic speeds J.Ae.Sci. Vol.14 No.10 p.567 October, 1947
9	Neilson	The effect of aspect ratio and taper on the pressure drag at supersonic speeds of unswept wings at zero lift NACA TN No.1487 November, 1947
10	Margolis	Effect of chordwise location of maximum thickness on the supersonic wave drag of sweptback wings NACA TN No.1543 March, 1948
11	Margolis	Supersonic wave drag of nonlifting sweptback tapered wings with Mach lines behind the line of maximum thickness NACA TN No.1672 August, 1948
12	Kainer	Theoretical calculations of the supersonic pressure distribution and wave drag for a limited family of tapered sweptback wings with symmetrical parabolic arc section at zero lift NACA TN No.2009 January, 1950
13	Multhopp and Winter	Charts for the calculation of the wave drag of swept wings RAE Tech Memo No. Aero 103 July, 1950
14	Nonweiler	Theoretical supersonic drag of non-lifting infinite span wings swept behind the Mach lines RAE Tech Note No. Aero 2073 (ARC 13,896) October, 1950.

REFERENCES (Contd.)

No.	Author	Title, etc.
15	Shaw	Analysis of theoretical results on the effect of section and taper on wing wave drag RAE Tech Memo No. Aero 144 December, 1950
16	Beane	The characteristics of wings having biconvex sections J.Ae.Sci. Vol.18 No.1 p.7 January, 1951
17	Chang	Applications of Von Karman's Integral method in supersonic wing theory NACA TN No.2317 March, 1951

Wt.2078.CP116.K3. Printed in Great Britain.

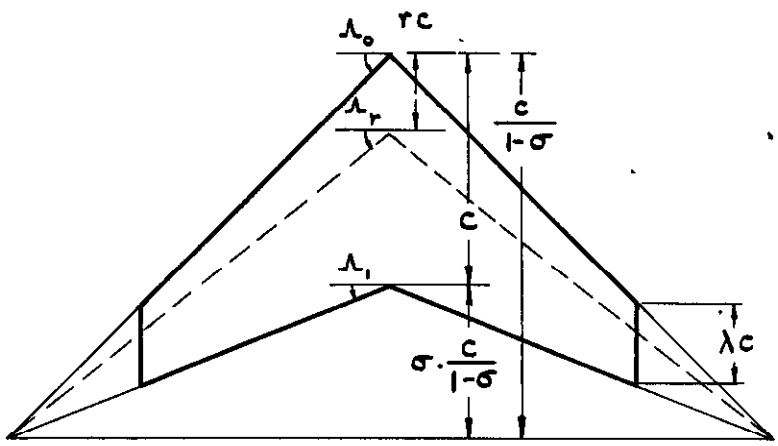

FIG.1. BASIC GEOMETRY OF A SWEPT TAPERED WING.

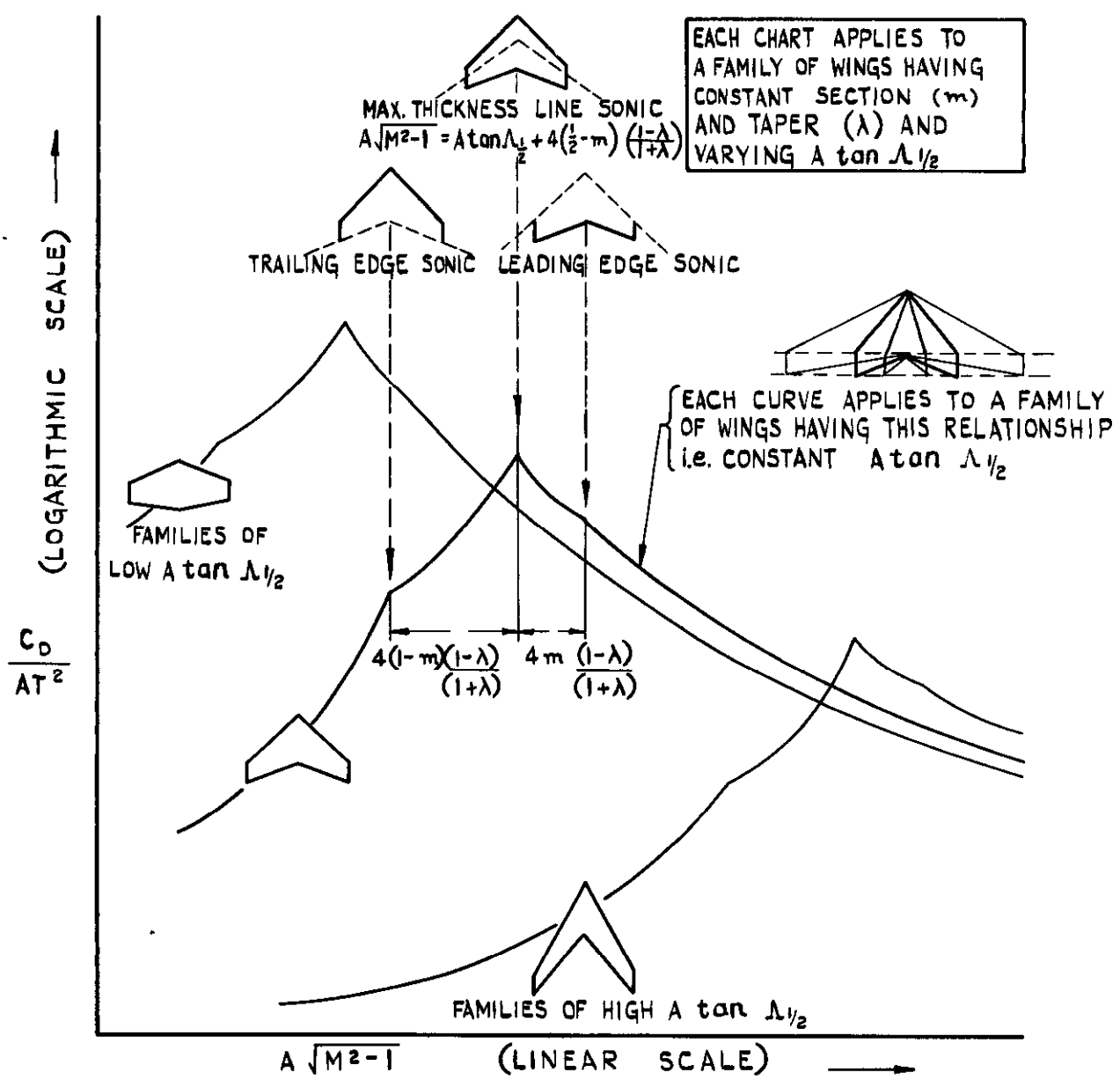

FIG.2. FUNDAMENTAL CHARACTERISTICS OF THE WAVE DRAG CURVES FOR A SWEPT WING OF DOUBLE WEDGE SECTION.

FIG.3(a).

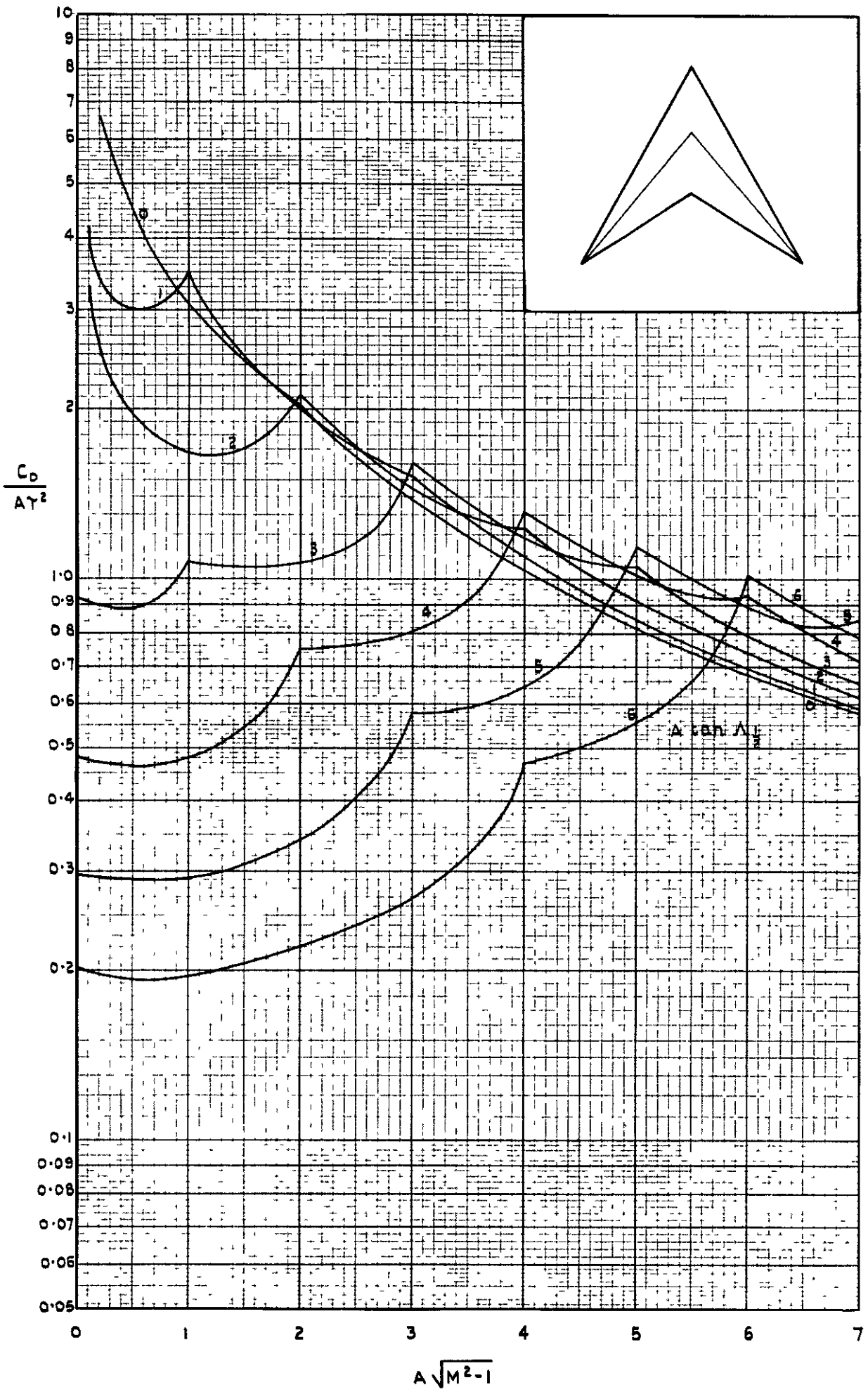

FIG.3(a). SUPERSONIC WAVE DRAG OF SYMMETRICAL DOUBLE WEDGE WINGS

$\lambda = 0$, $m = 0{\cdot}5$.

FIG.3(b).

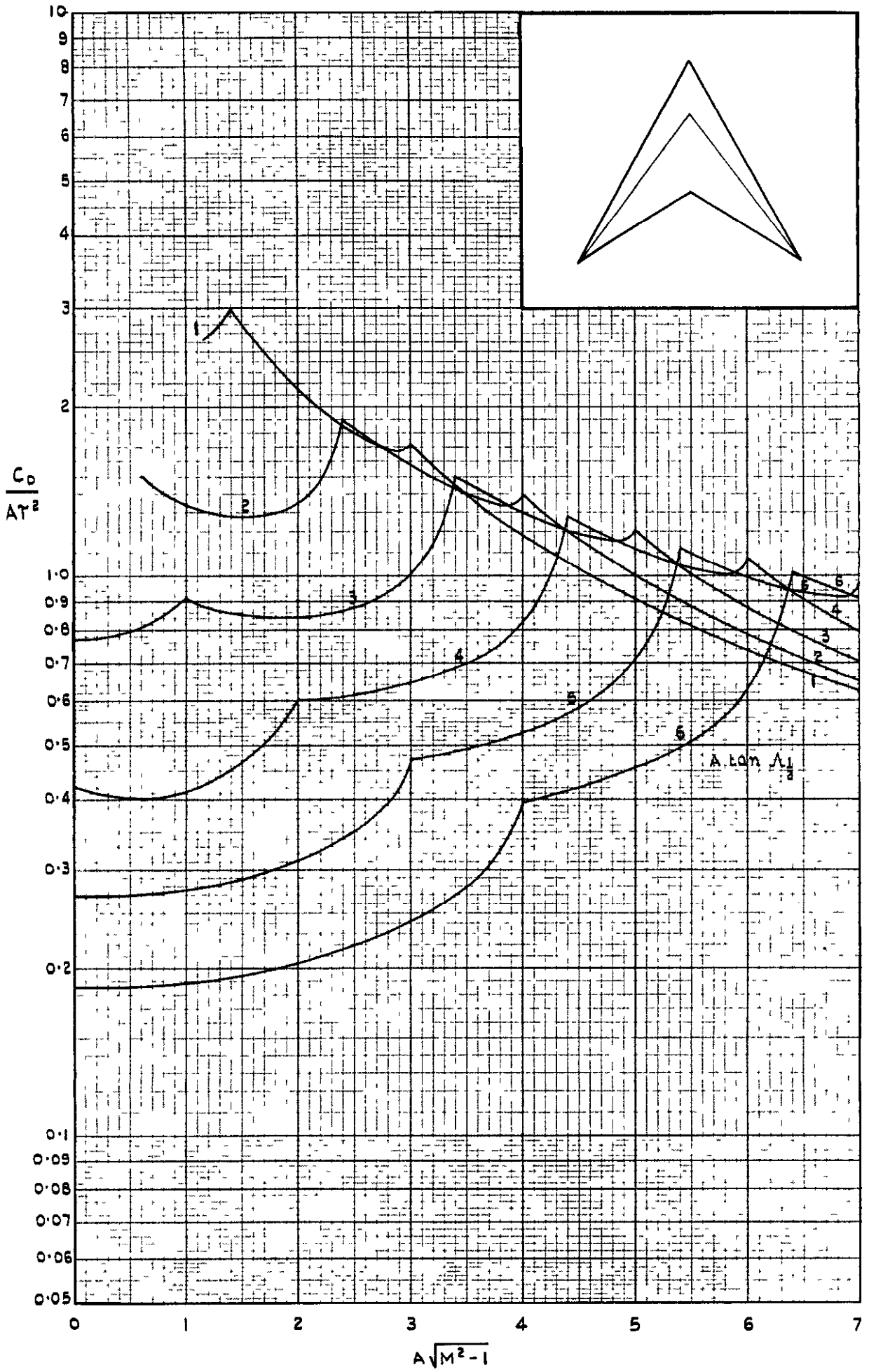

FIG.3(b). SUPERSONIC WAVE DRAG OF SYMMETRICAL DOUBLE WEDGE WINGS

$\lambda = 0$, $m = 0 \cdot 4$.

FIG.3 (c).

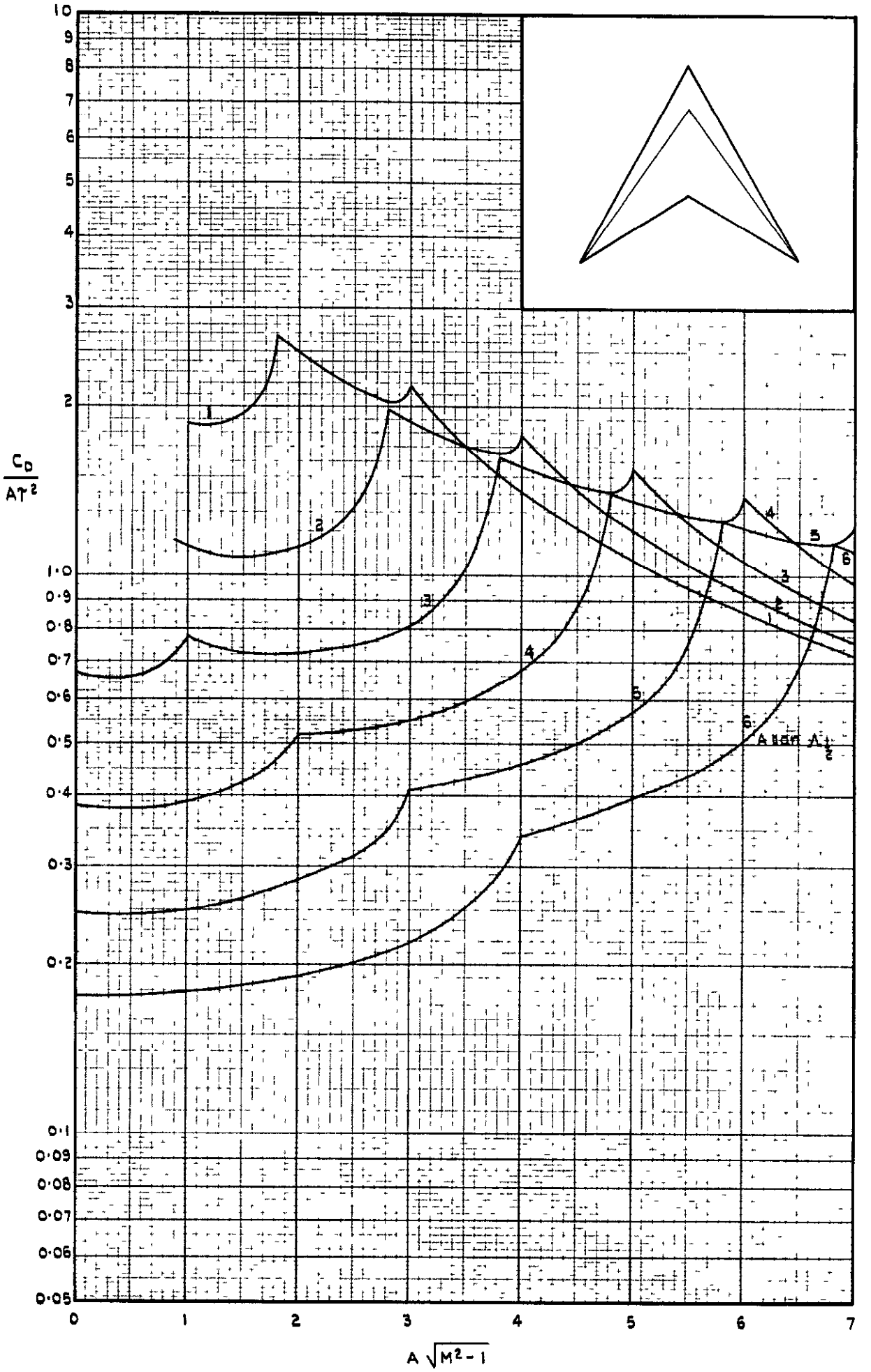

FIG.3 (c). SUPERSONIC WAVE DRAG OF SYMMETRICAL DOUBLE WEDGE WINGS

$\lambda = 0$, $m = 0 \cdot 3$.

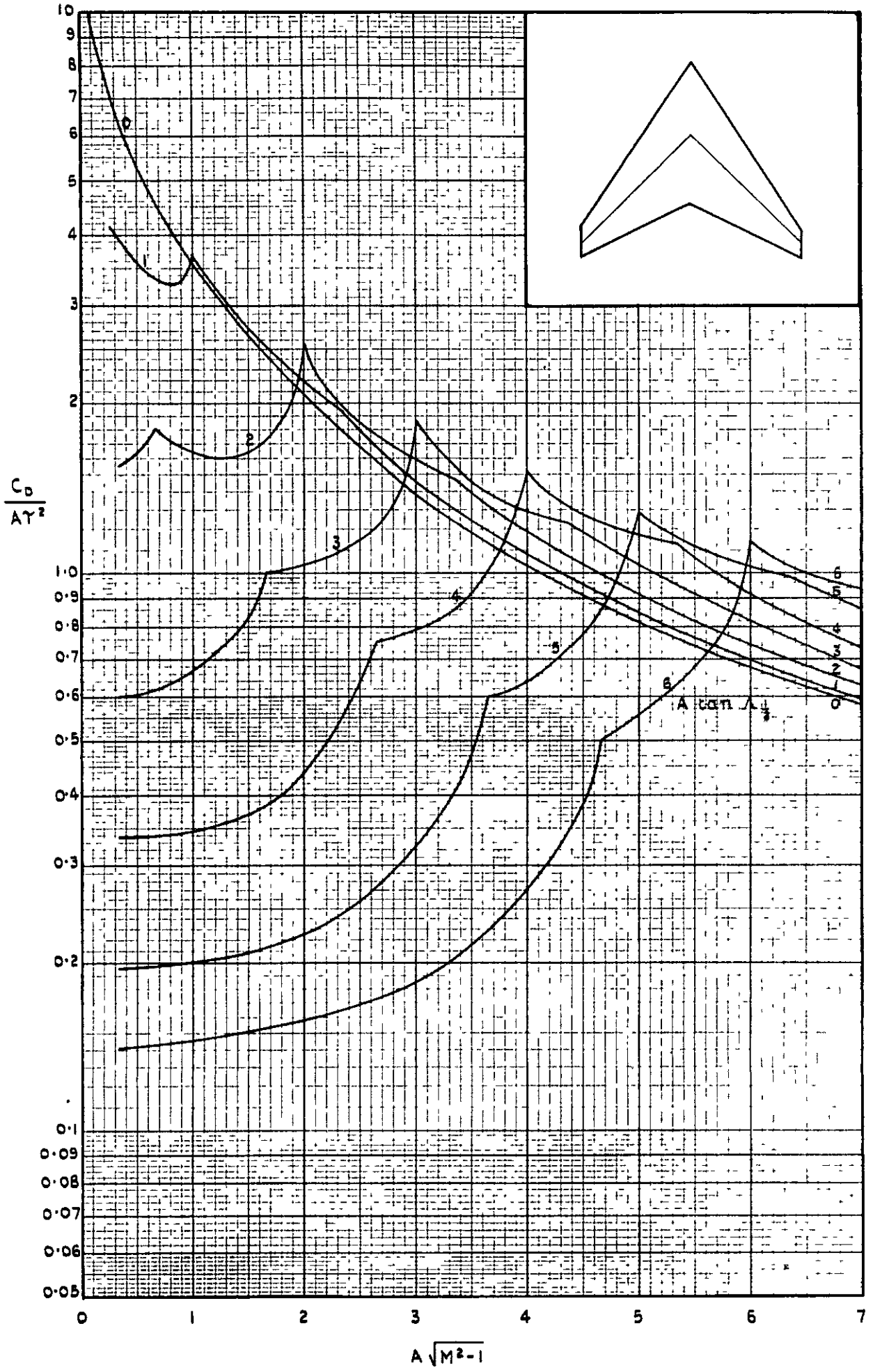

FIG.4. SUPERSONIC WAVE DRAG OF SYMMETRICAL DOUBLE WEDGE WINGS

$\lambda = 0{\cdot}2$, $m = 0{\cdot}5$.

FIG.5.

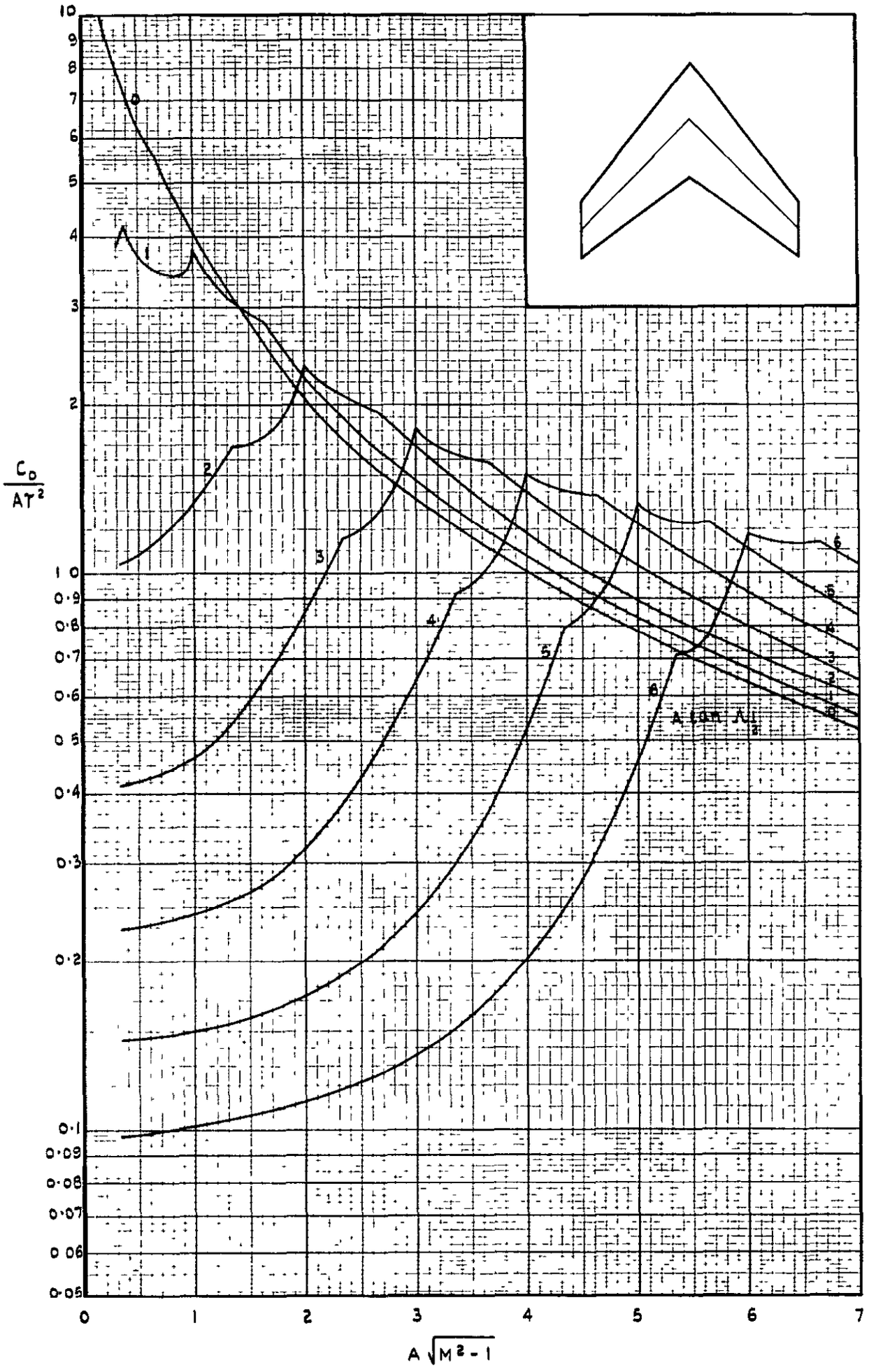

FIG.5. SUPERSONIC WAVE DRAG OF SYMMETRICAL DOUBLE WEDGE WINGS

$\lambda = 0{\cdot}5$, $m = 0{\cdot}5$.

FIG.6(a).

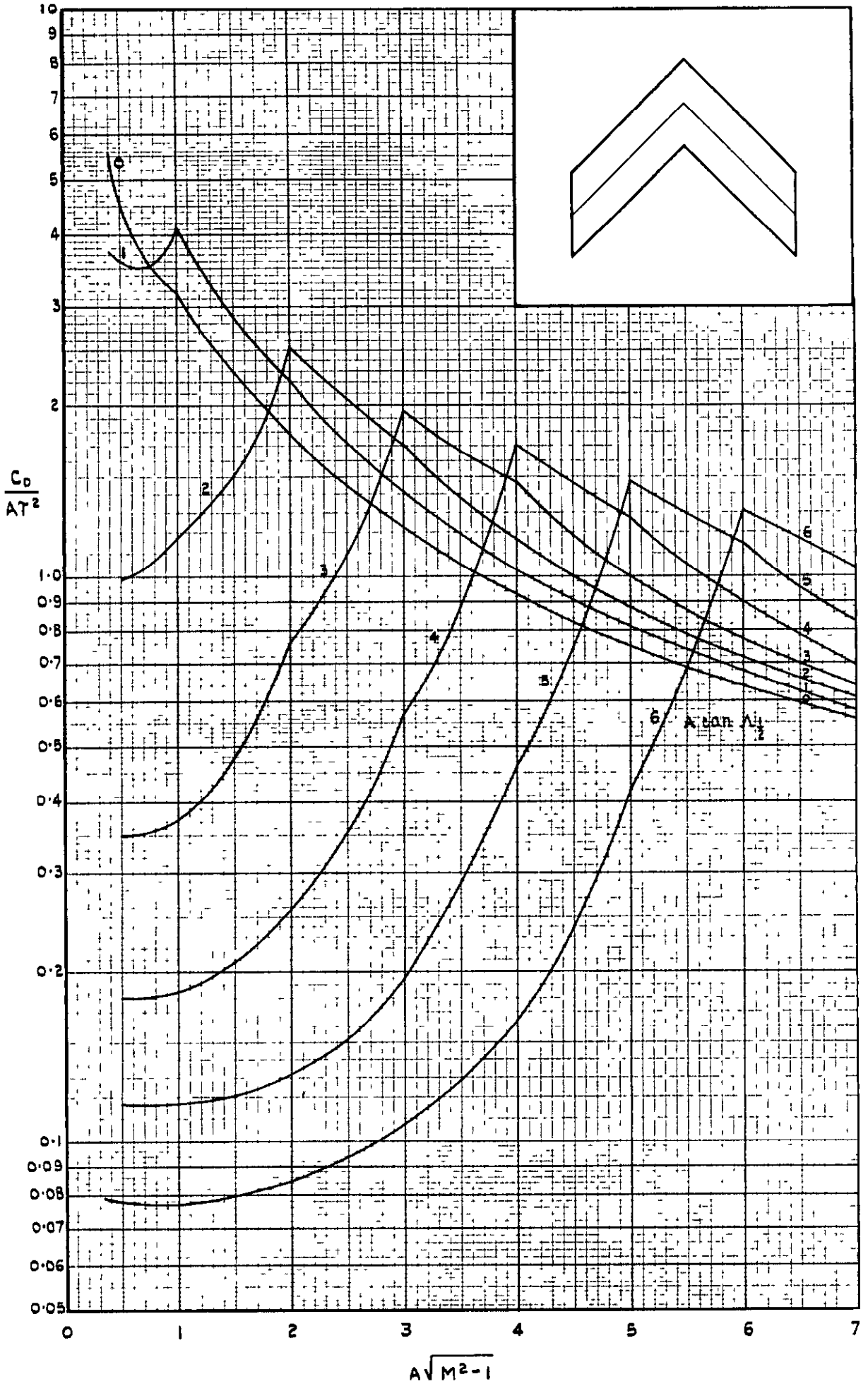

FIG.6(a). SUPERSONIC WAVE DRAG OF SYMMETRICAL DOUBLE WEDGE WINGS $\lambda = 1{\cdot}0$, $m = 0{\cdot}5$.

FIG.6 (b).

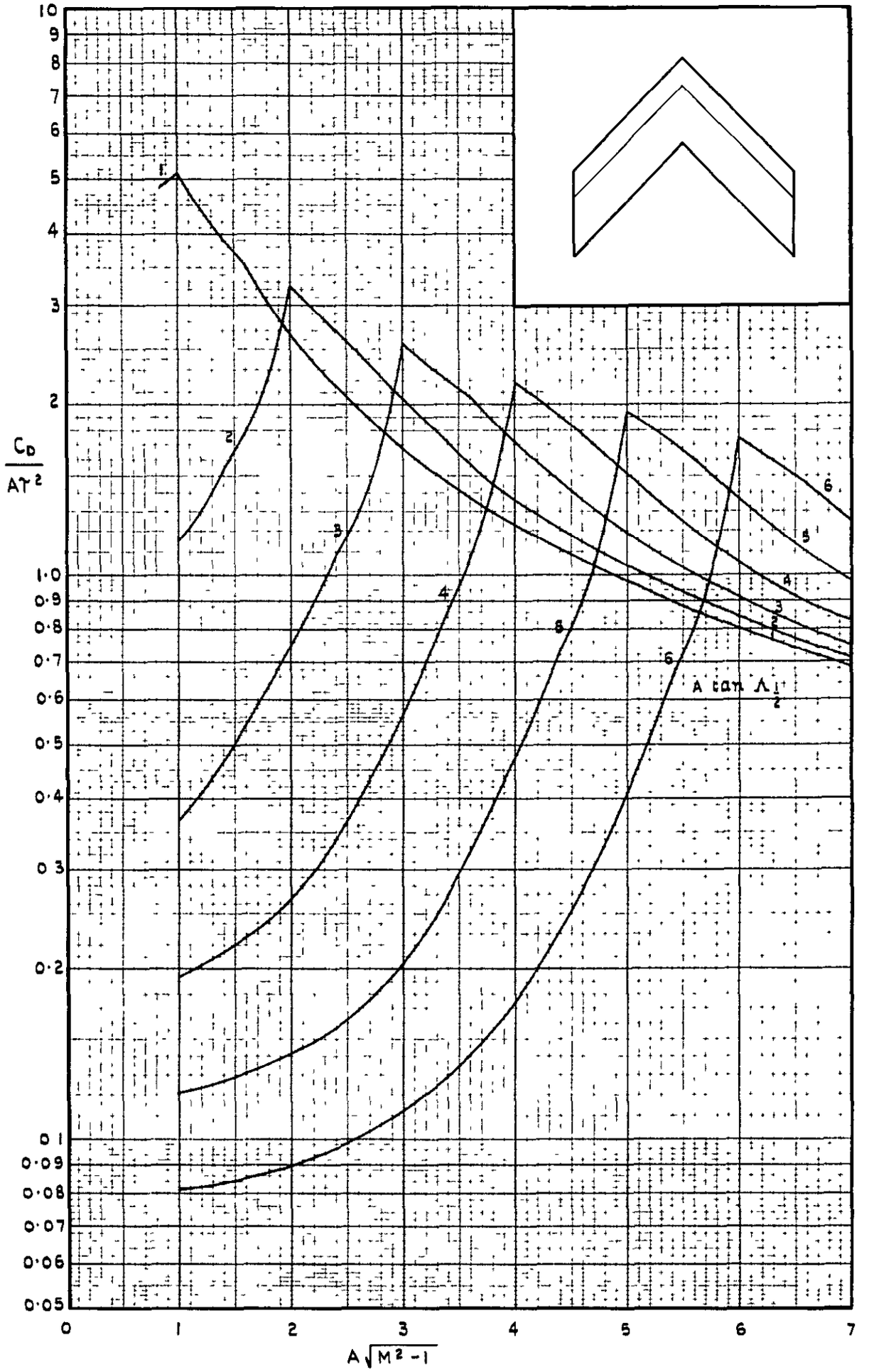

FIG.6(b). SUPERSONIC WAVE DRAG OF SYMMETRICAL DOUBLE WEDGE WINGS

$\lambda = 1{\cdot}0$, $m = 0{\cdot}3$.

FIG. 7.

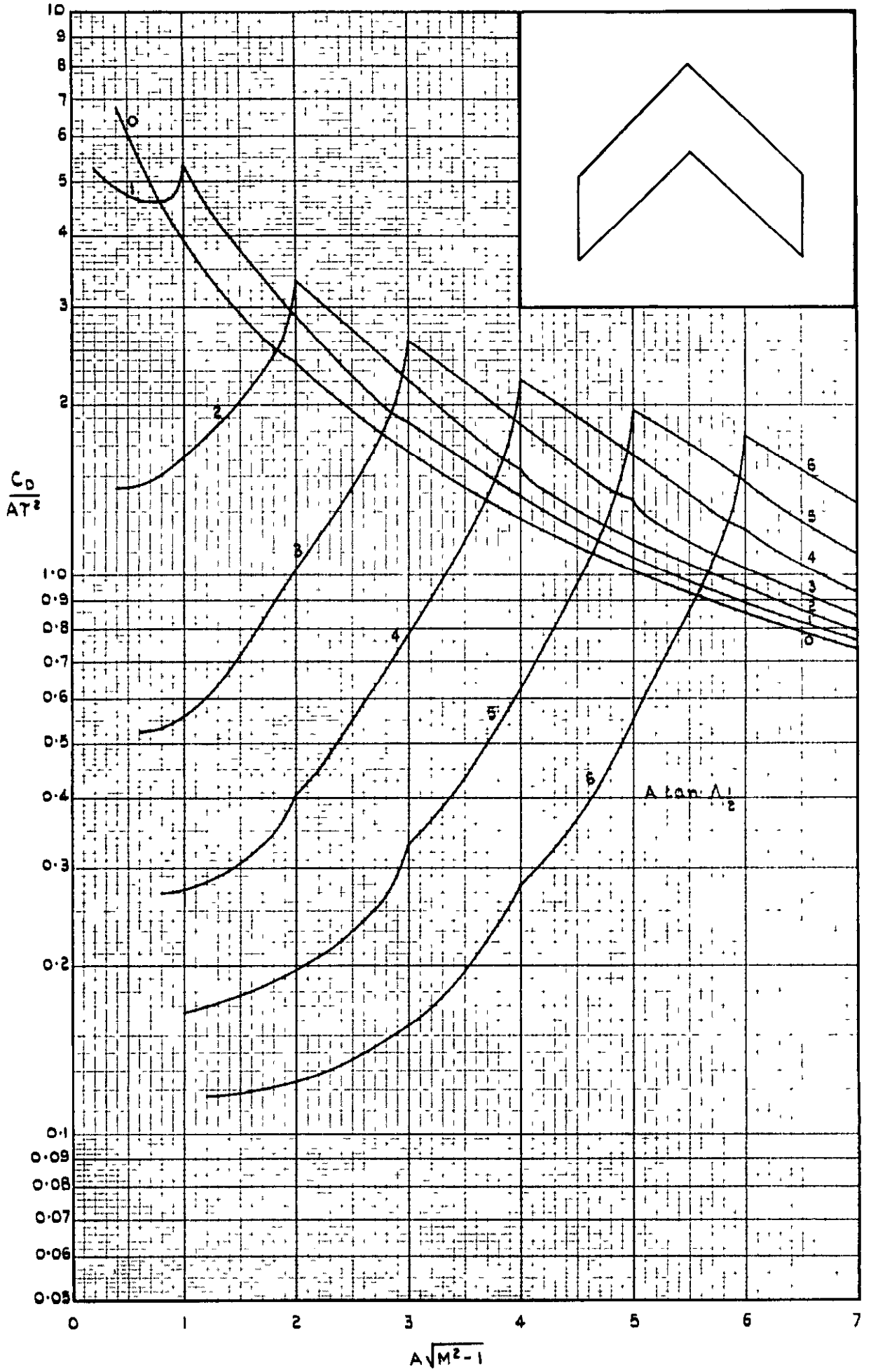

FIG. 7. SUPERSONIC WAVE DRAG OF BICONVEX PARABOLIC ARC WINGS

$\lambda = 1$.

FIG.8.

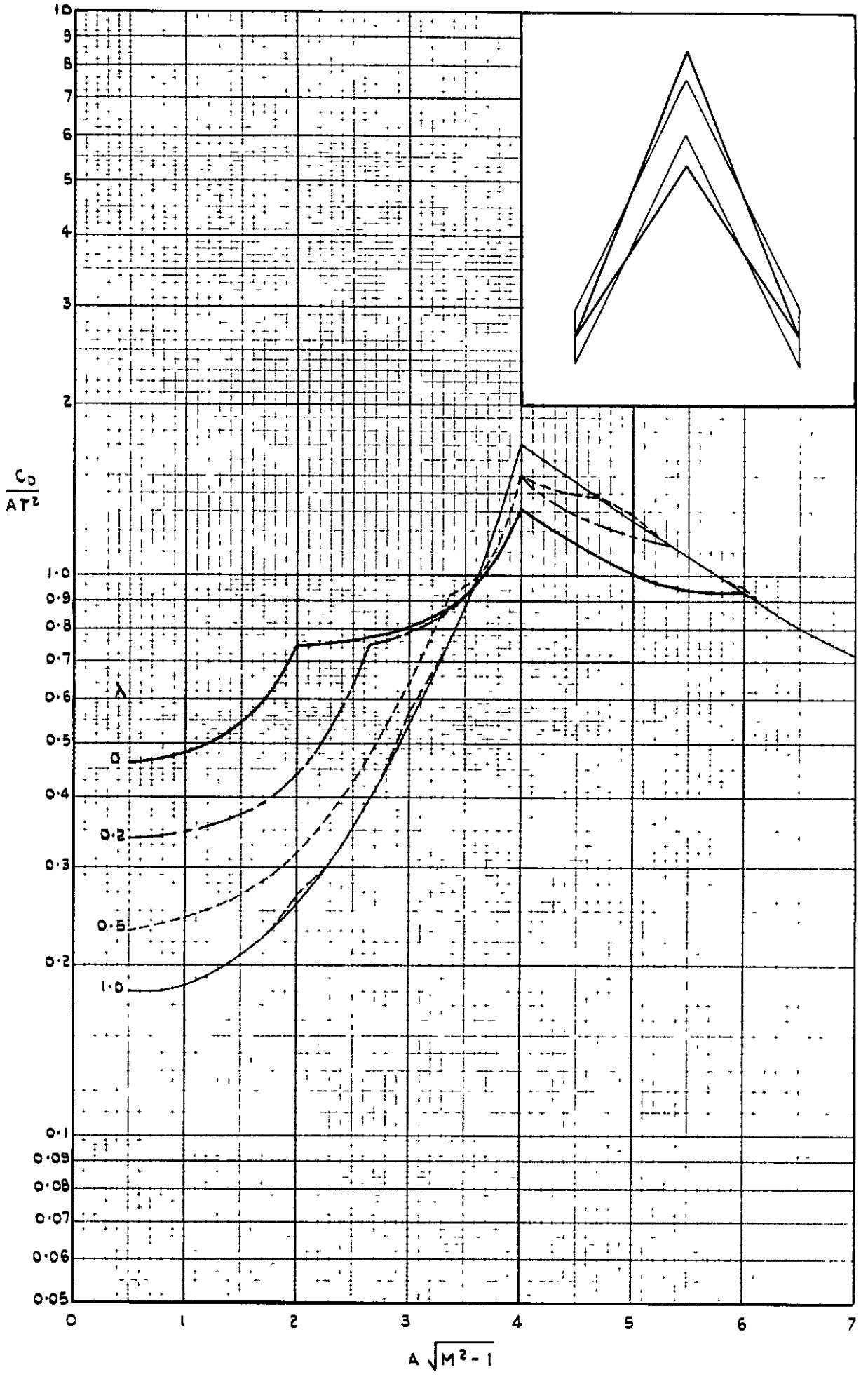

FIG.8. EFFECT OF TAPER ON THE SUPERSONIC WAVE DRAG OF SYMMETRICAL DOUBLE WEDGE WINGS.

$A \tan \Lambda_{\frac{1}{2}} = 4$, $m = 0{\cdot}5$.

FIG. 9(a).

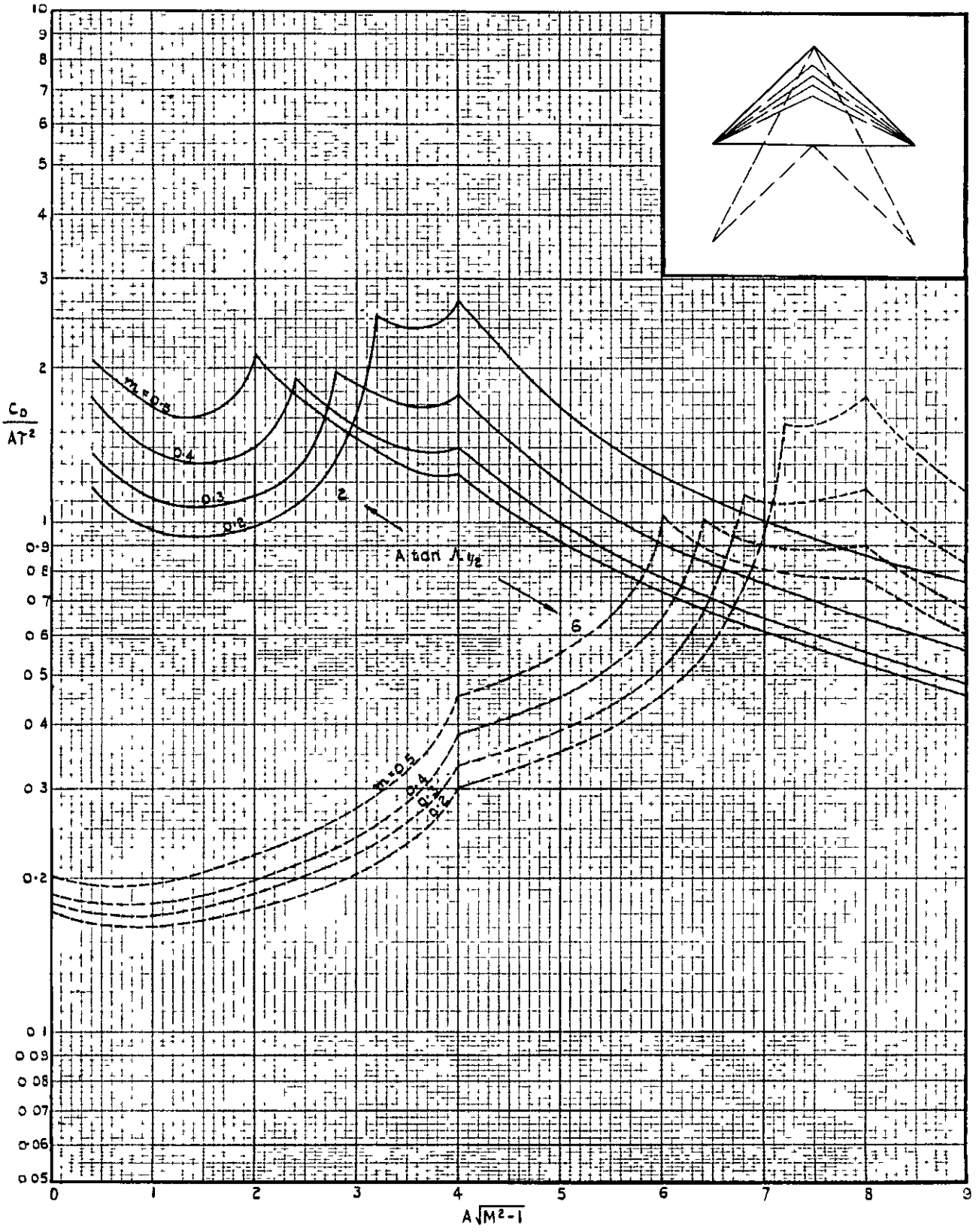

FIG. 9 (a). EFFECT OF MAXIMUM THICKNESS POSITION ON THE SUPERSONIC WAVE DRAG OF DOUBLE WEDGE WINGS.

$\lambda = 0$.

FIG.9(b).

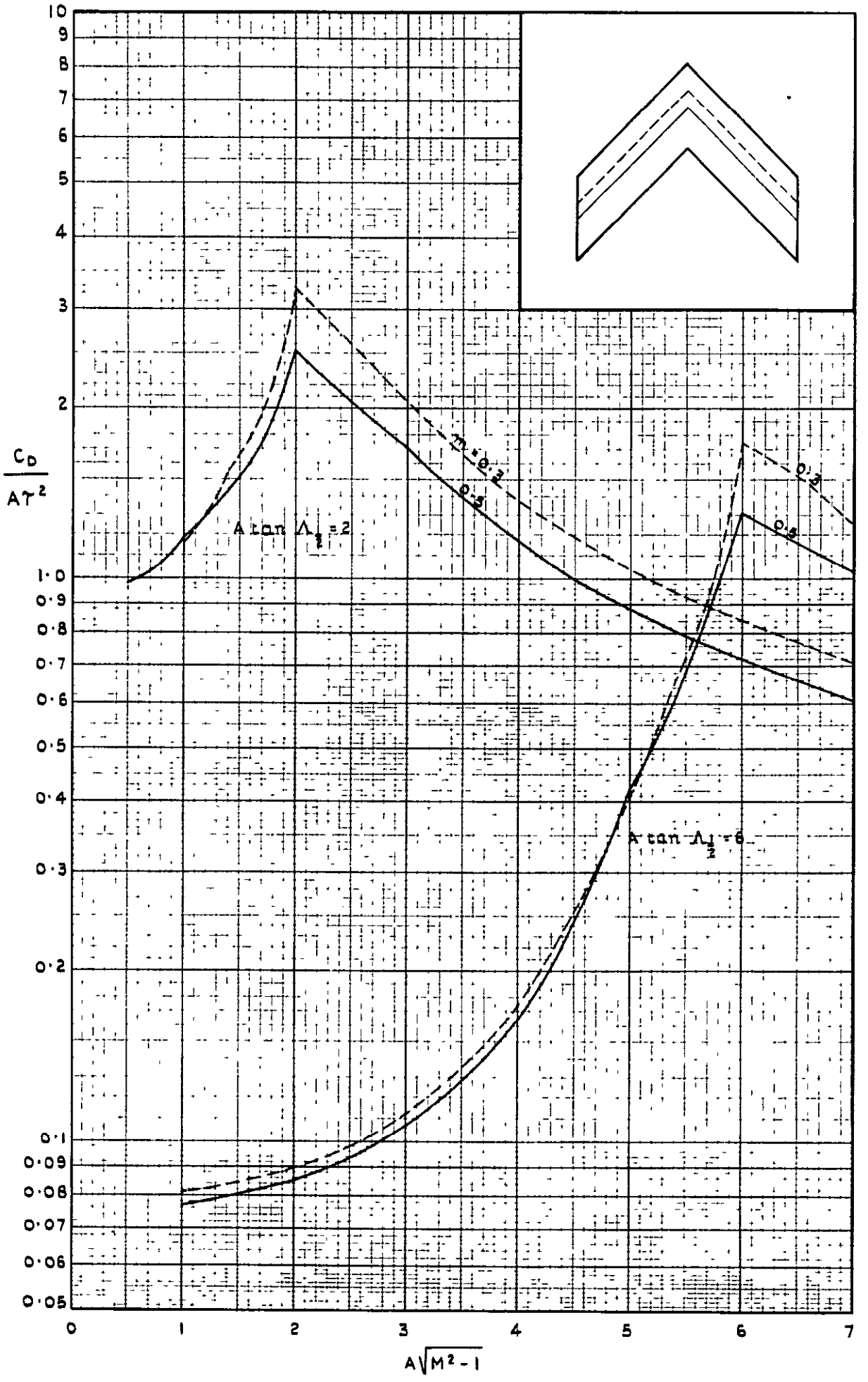

FIG.9(b). EFFECT OF MAXIMUM THICKNESS POSITION ON THE SUPERSONIC WAVE DRAG OF DOUBLE WEDGE WINGS

$\lambda = 1{\cdot}0$.

C.P. No. 116
(15,595)
A.R.C. Technical Report

PUBLISHED BY HER MAJESTY'S STATIONERY OFFICE

To be purchased from

York House, Kingsway, LONDON, W.C.2: 423 Oxford Street, LONDON, W.1
P.O. Box 569, LONDON, S.E 1
13a Castle Street, EDINBURGH, 2 | 1 St Andrew's Crescent, CARDIFF
39 King Street, MANCHESTER, 2 | Tower Lane, BRISTOL, 1
2 Edmund Street, BIRMINGHAM, 3 | 80 Chichester Street, BELFAST
or from any Bookseller

1953

Price 3s. 6d. net

PRINTED IN GREAT BRITAIN

S.O. Code No. 23-9007-16